

## Structure and Dynamics of Colliding Plasma Jets

C. K. Li,<sup>1,\*</sup> D. D. Ryutov,<sup>2</sup> S. X. Hu,<sup>3</sup> M. J. Rosenberg,<sup>1</sup> A. B. Zylstra,<sup>1</sup> F. H. Séguin,<sup>1</sup> J. A. Frenje,<sup>1</sup>  
D. T. Casey,<sup>1,†</sup> M. Gatu Johnson,<sup>1</sup> M. J.-E. Manuel,<sup>1,‡</sup> H. G. Rinderknecht,<sup>1</sup> R. D. Petrasso,<sup>1</sup> P. A. Amendt,<sup>2</sup>  
H. S. Park,<sup>2</sup> B. A. Remington,<sup>2</sup> S. C. Wilks,<sup>2</sup> R. Betti,<sup>3</sup> D. H. Froula,<sup>3</sup> J. P. Knauer,<sup>3</sup> D. D. Meyerhofer,<sup>3</sup>  
R. P. Drake,<sup>4</sup> C. C. Kuranz,<sup>4</sup> R. Young,<sup>4</sup> and M. Koenig<sup>5</sup>

<sup>1</sup>*Plasma Science and Fusion Center, Massachusetts Institute of Technology, Cambridge, Massachusetts 02139, USA*

<sup>2</sup>*Lawrence Livermore National Laboratory, Livermore, California 94550, USA*

<sup>3</sup>*Laboratory for Laser Energetics, University of Rochester, Rochester, New York 14623, USA*

<sup>4</sup>*University of Michigan, Ann Arbor, Michigan 48109, USA*

<sup>5</sup>*Laboratoire pour l'Utilisation des Lasers Intenses, UMR 7605, CNRS-CEA-Université Paris VI-Ecole Polytechnique, 91128 Palaiseau Cedex, France*

(Received 24 August 2013; published 3 December 2013)

Monoenergetic-proton radiographs of laser-generated, high-Mach-number plasma jets colliding at various angles shed light on the structures and dynamics of these collisions. The observations compare favorably with results from 2D hydrodynamic simulations of multistream plasma jets, and also with results from an analytic treatment of electron flow and magnetic field advection. In collisions of two noncollinear jets, the observed flow structure is similar to the analytic model's prediction of a characteristic feature with a narrow structure pointing in one direction and a much thicker one pointing in the opposite direction. Spontaneous magnetic fields, largely azimuthal around the colliding jets and generated by the well-known  $\nabla T_e \times \nabla n_e$  Biermann battery effect near the periphery of the laser spots, are demonstrated to be “frozen in” the plasma (due to high magnetic Reynolds number  $Re_M \sim 5 \times 10^4$ ) and advected along the jet streamlines of the electron flow. These studies provide novel insight into the interactions and dynamics of colliding plasma jets.

DOI: [10.1103/PhysRevLett.111.235003](https://doi.org/10.1103/PhysRevLett.111.235003)

PACS numbers: 52.30.-q, 52.38.Fz, 52.72.+v

We report on recent experiments for studying the collisions of two identical plasma jets generated by high-power lasers. The observations have, for the first time, shown key aspects of jet collisions at various angles. In particular, it was seen that plasma flowing into the collision from the two jets forms a stagnation surface along which incoming electrons flow away from the collision. This surface is a plane that bisects the angle formed by the two jets (the “bisector plane”). This and other observations are combined with numerical simulations and analytic models, reinforcing our insight into the interactions of colliding plasma jets.

The collision of high-Mach-number plasma jets in the laboratory is attracting increasing attention since such interactions can be used as a test bed for studying many astrophysical phenomena and basic physics problems in self-organization [1–4]. Exploring the spatial structure and temporal evolution of these colliding jets, as well as their relationship with self-generated electromagnetic fields [5–8], is of essential importance for understanding the underlying physics of plasma jet interactions [9,10].

Although they have very different spatial, temporal, temperature and density scales, laboratory-generated plasma jets and astrophysical jets share a large variety of hydrodynamic similarities [11–18]. As indicated by numerous dimensionless parameters, these similarities suggest common physical processes that govern jet dynamics and allow

us to scale laboratory jets to astrophysical conditions under some circumstances [9–18]. For example, recent experiments [2,3,19] and numerical simulations [20] indicate that the collisions of two counterstreaming plasma flows with sufficiently large spatial overlap lead to collisionless shocks mediated by the development of plasma microturbulence [21,22]. Such shocks can be scaled to mimic and explain many astrophysical phenomena [2–4,9–22]. To simulate aspects of accretion disks and outflows in astrophysics, an array of properly directed plasma jets has been proposed [23,24] to drive and form a differentially rotating, quasi-planar disc in which an azimuthal magnetic field, seeded with a cusp magnetic configuration, will be enhanced. The interactions among these jets in such a specially configured plasma will play a critical role in reproducing this particular astrophysical phenomenon [23,24]. In inertial confinement fusion (ICF) [25], the relevance of plasma jet interactions is evident in the plasma stagnation on a hohlraum axis, which is critical to hohlraum x-ray drive symmetry and ICF capsule implosions [25,26].

Laser-produced colliding jets can be supersonic [11–13,27,28], with sufficiently high kinetic energies that collisions of ions in one jet with ions in another jet are negligible. In this case, the ion streams interpenetrate each other freely [1,29]. The electrons, whose thermal velocity is much higher than the flow velocity, form a background common to both streams. Since the electrons have a

temperature that is lower than the ion directed energy by a factor  $\sim 50$ – $100$ , they are highly collisional. The average velocity of the electrons is established to provide quasi-neutrality. After two equal-strength jets collide, their electrons all turn and flow away along the bisector plane. This picture cannot be adequately described by standard hydrodynamics.

The experiments, illustrated schematically in Fig. 1, were performed at the OMEGA Laser Facility [30]. V-shaped targets [31,32] were constructed with two  $50\text{-}\mu\text{m}$ -thick,  $3\text{ mm} \times 3\text{ mm}$  plastic (CH) foils which have a full opening angle of  $60^\circ$ . Each foil was driven by two laser beams ( $0.351\text{ }\mu\text{m}$  in wavelength) at an angle  $\sim 28^\circ$  to the foil normal, toward the axis of the four-foil two-beam setup. Each beam had total energy  $\sim 500\text{ J}$  during a 1-ns square pulse, with full spatial and temporal smoothing [33]. A plasma plume was generated on each foil by laser ablation. When the plumes from the two adjacent foils collided they generated a plasma jet. The jet tip moving velocity is estimated using time-of-flight measurements to be  $V_j \sim 1700\text{ km s}^{-1}$ , indicating jet propagation is supersonic with internal Mach number  $M \sim 10$  or greater. Two such jets, from identical targets

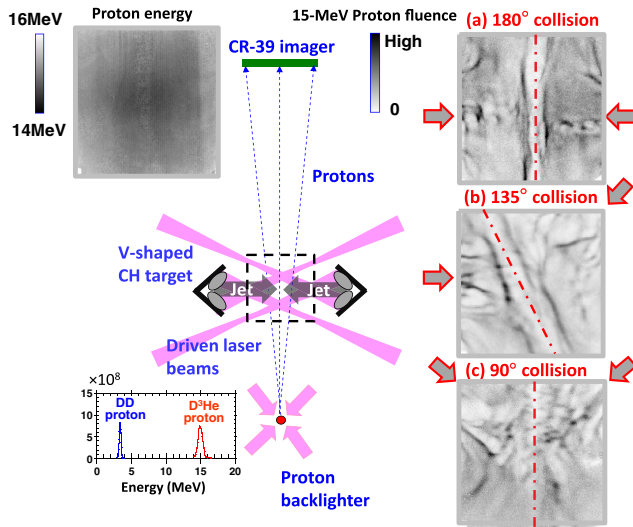


FIG. 1 (color online). Schematic diagram of the experimental setup. The proton backlighter (imploded  $\text{D}^3\text{He}$ -filled thin-glass-shell capsule driven by 30-OMEGA laser beams) is typically 1 cm from the collision region and has the illustrated monoenergetic spectra from the reactions  $\text{D} + {}^3\text{He} \rightarrow \alpha + p$  (14.7 MeV) and  $\text{D} + \text{D} \rightarrow \text{T} + p$  (3.0 MeV). The typical backlighter spatial and temporal resolutions are  $\sim 40\text{ }\mu\text{m}$  and  $\sim 80\text{ ps}$ , respectively [43]. Sample images of proton fluence, taken with 15-MeV  $\text{D}^3\text{He}$  protons at  $\sim 4\text{ ns}$  from the onset of the laser drive on the V-shaped targets at different angles, are shown. The dashed-dotted lines shown in the images indicate the bisector planes for various cases. The dashed square indicates the field of view of the C39 proton detector, but shown as if it were rotated  $90^\circ$  into the plane of the diagram. The distance from the sample region to the detector is 27 cm.

(distance between each target tip and the central collision region is 0.5 cm), collided with each other when they met at the bisector plane. Radiographs of jet collisions at angles of  $180^\circ$ ,  $135^\circ$ , and  $90^\circ$ , made with 15-MeV protons [34–36], are shown in Figs. 1(a)–1(c).

A common and striking feature in these images is the “flattened” (quasiplanar) region along the bisector planes, with low proton fluence inside, but surplus protons on the edges. Plasma expansion perpendicular to the bisector plane is minimized because the plasma there reaches a balance between the continuous arrival of new jet material and the outflow of plasma along the bisector plane. Such a fluence structure cannot be caused by plasma scattering because the Coulomb scattering of these backlighting protons is negligible, as shown by the proton energy image in Fig. 1 [37]. The apparently flattened, low-proton-fluence region thus formed in the fluence images must be a consequence of proton deflection by fields on each side of the bisector plane with opposite directions. We note that the radiography method fortuitously gives strong contrast between the image feature associated with the bisector plane and the more subtle image features associated with the jets themselves in the regions between their sources and the bisector plane [38].

For uniquely determining the types of fields, Fig. 2 gives lineouts crossing the flattened regions in the center of the images for two proton energies. The small-angle deflection of backlighter protons by fields in the plasma, which is what forms structures in the images, is measured as the proton displacement in the detector plane ( $\xi$ ) divided by the distance from plasma to detector ( $A-a$ ). Because of the Lorentz force [ $\mathbf{F} = e(\mathbf{E} + \mathbf{v} \times \mathbf{B})$ ], deflection by electric fields is proportional to the inverse of the proton energy  $\varepsilon_p^{-1}$ , while deflection by magnetic fields is proportional to  $\varepsilon_p^{-1/2}$ . The ratio of the measured widths (FWHM) in this region for 3.3- and 15-MeV protons is  $\sim 1.8$ , a number that

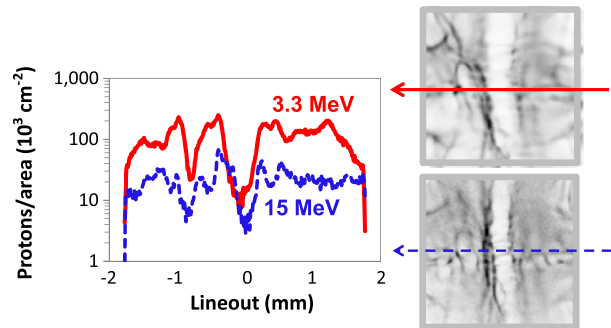


FIG. 2 (color online). Lineouts from images taken at  $\sim 4.7\text{ ns}$  with 15 and 3.3 MeV protons from head-on collisions of two plasma jets are shown. The solid and dashed profiles correspond to the solid and dashed straight lines in the images, indicating the different energies of the backlighting protons. The ratio of the widths of the flattened region demonstrates the dominant role of magnetic field in forming such a structure.

is close to the square root of the proton energy ratio of  $(15/3.3 \text{ MeV})^{1/2} \sim 2.1$ , strongly suggesting that the dominant source for proton deflections is magnetic fields rather than electric fields ( $15/3.3 \text{ MeV} \sim 4.6$ ). These fields must have dominant azimuthal components (around the jet axis) and their strength is estimated by

$$\int \mathbf{B} \times d\ell = -\frac{Am_p V_p \xi}{q(A-a)a}, \quad (1)$$

where  $a = 1 \text{ cm}$  and  $A = 28 \text{ cm}$ ;  $m_p$  is proton mass and  $V_p$  is proton velocity;  $q$  is the proton electric charge, and  $d\ell$  is the differential pathlength along the proton trajectory. From Fig. 2, we obtain  $|\int \mathbf{B} \times d\ell| \sim 15 \text{ T cm}$ . Taking the scale size as the diameter of the flattened disk (from a 3D configuration)  $\geq 0.5 \text{ cm}$  (slightly larger than the field of view of our detector), results in a magnetic field roughly of an order  $\sim 30 \text{ T}$ . Note that the magnetic deflection of the carbon and hydrogen ions of the streams has an opposite sign on the two sides of the bisector plane. For fields weaker than  $\sim 30 \text{ T}$  a mutual neutralization of the deflections may occur, restoring a simple conical ion flow in each of the jets.

The head-on collisions were simulated with the two-dimensional (2D) hydrodynamic code [39,40]. Figure 3 displays postprocessed snapshots showing the spatial structure and temporal evolution of two counterstreaming plasma jets colliding with each other. The numerical simulation and Thomson scattering measurements [41] indicate

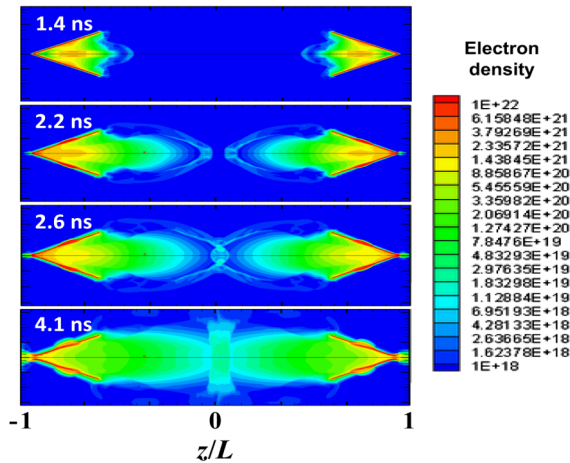


FIG. 3 (color online). 2D DRACO hydrodynamic simulations of the two head-on plasma jets which displays the jets' formation at  $t \approx 1.4 \text{ ns}$ ; propagation at  $t \approx 2.2 \text{ ns}$  (a clear bow shock structure is seen in front of the jets); the onset of plasma flow in the transverse direction, and the formation of a high-pressure region in the bisector plane, at  $t \approx 2.6 \text{ ns}$ ; and the transverse expansion of the high-pressure region in the bisector plane  $t \approx 4.1 \text{ ns}$ . In this simulation, a low density ( $\sim 2 \times 10^{-6} \text{ g cm}^{-3}$ ) deuterium gas has been added to the background. The simulation of plasma flow (4.1 ns) appears to be quite consistent with the shape of the proton deflection images shown in Figs. 1 and 2.

that the electron flow stagnates in the axis and subsequently spreads sideways, forming a flattened region (a disk in 3D view) with typical  $n_e \sim 10^{19}\text{--}10^{20} \text{ cm}^{-3}$  and  $T_e \sim 500\text{--}1000 \text{ eV}$ .

To place the discussions in the broader context of basic plasma physics, Table I gives physical parameters for the head-on collisions. The long jet-jet ion mean-free path indicates that the interjet ion-ion collisions are essentially collisionless. The general picture of the magnetic field being frozen into the electron fluid and advected along its streamlines is only to be expected if the magnetic Reynolds number is high, and the estimated magnetic Reynolds number of Table I is gratifyingly large. Note that the carbon gyroradius is comparable to or even smaller than the size of the observed structures, indicating that the regular azimuthal field may cause the ions to be deflected from their initial straight trajectories, create radial ion flow in both jets, significantly affecting the ion dynamics near the bisector plane. This happens despite the fact that the magnetic pressure  $p_M$  of the 30 T field, as estimated from the measurements, is orders of magnitude smaller than the ram pressure  $\rho v^2$  of either of the jets:  $p_M/\rho v^2 \sim 2 \times 10^{-3}$ . The presence of the two counterpropagating streams makes this effect possible.

The generation and advection of spontaneous magnetic fields are described by the Faraday equation combined with a simplified version of the generalized Ohm's law:  $\partial \mathbf{B} / \partial t = \nabla \times (\mathbf{u} \times \mathbf{B}) + \mathbf{S}$  [9] whose azimuthal component  $B_\varphi$  is given in the cylindrical coordinate as

$$\frac{\partial B_\varphi}{\partial t} = \frac{\partial}{\partial r}(B_\varphi u_r) - \frac{\partial}{\partial z}(B_\varphi u_z) + S_\varphi, \quad (2)$$

where  $u_r$  ( $u_z$ ) is the radial (axial) component of the velocity of electron flow [1], and  $S_\varphi$  is the source term for the field generation, which is dominated by the so-called Biermann battery effect ( $\nabla n_e \times \nabla T_e$ ). The frozen-in condition for the azimuthal field in axisymmetric effective flow is [1]

$$B_\varphi / n_e r = \text{const}. \quad (3)$$

This suggests that there exists a zone near the bisector plane from which the plasma electron flow becomes almost

TABLE I. Calculated parameters of two interpenetrating jets based on  $v = 1.7 \times 10^8 \text{ cm s}^{-1}$ ,  $T_e \sim 1 \text{ keV}$ ,  $n_C \sim 4 \times 10^{18} \text{ cm}^{-3}$  (per jet), length scale of the overlap region  $l \sim 0.3 \text{ cm}$ , and strength of magnetic field  $\sim 30 \text{ T}$ .

Parameters	
Carbon ion energy ( $W_C$ )	175 keV
Carbon ion gyroradius ( $r_G$ )	0.8 mm
Jet-jet ion mean-free path ( $\lambda_{ZZ}$ )	20 cm
$e$ - $e$ collision frequency ( $\nu_{ee}$ )	$3 \times 10^{10} \text{ s}^{-1}$
Dynamic time ( $t = l/v$ )	$1.75 \times 10^{-9} \text{ s}$
Magnetic diffusivity ( $D_M$ )	$10^3 \text{ cm}^2 \text{ s}^{-1}$
Magnetic Reynolds number ( $\text{Re}_M$ )	$5 \times 10^4$

radial, and the increasing plasma density due to contributions from the other jet would lead to the increase of magnetic fields as this flow spreads sideways, which is consistent with the observations (Fig. 1).

The streamlines of electron flow are modeled with a modification of an analytical description of head-on collisions [1], where the flow follows a solution of the differential equation

$$\frac{dr}{u_r} = \frac{dz}{u_z} \tag{4}$$

in cylindrical coordinates, and the velocities  $u_r$  and  $u_z$  are given by Eqs. (21) and (22) of Ref. [1], respectively. Near each target, the flow is diverging and the frozen-in Biermann battery field decreases along the streamlines. Shown in Fig. 4(c), the “conical” streamlines approach from both sides, stagnate, and subsequently spread sideways, indicating the electron flow stagnates near the bisector plane, and the magnetic field is recompressed to a quasiplanar structure [1,42]. The bisector plane acts as an impermeable boundary for electron fluid, and the recompressed field has an opposite handedness in the opposite flows. By virtue of the frozen-in condition, the streamlines deviate toward much larger radii subsequent to the stagnation, leading to enhanced magnetic fields due to increasing products of density and radius [Eq. (3)]. These processes produce a flattened structure along the bisector plane and mimic the observed Fig. 4(a) and simulated Fig. 4(b) structure.

To model the noncollinear collisions at an arbitrary angle, which are more generally relevant to those occurring in nature than collisions of perfectly collinear jets, a Cartesian coordinate system is more convenient because the azimuthal symmetry is broken [Fig. 5(a)]. Normalizing

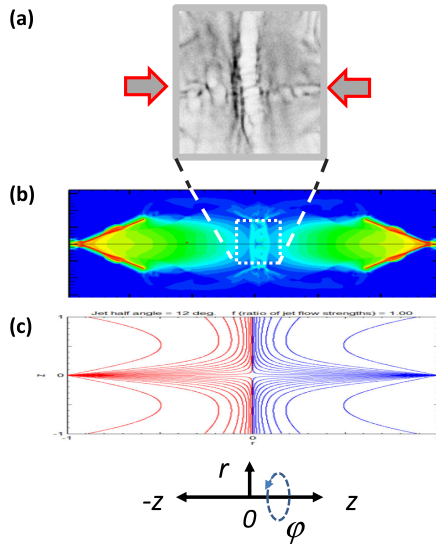


FIG. 4 (color online). Proton image (a), numerical simulation (b), and analytical model (c) of streamlines of electron “effective flow” for collisions of two counterstreaming plasma jets (head-on).

the distances to the parameter  $L$  (half distance between the targets), an equation for the streamlines can be written as

$$\begin{aligned} & \arctan\left(\frac{1}{\phi_1} \arctan\frac{y}{x}\right) \\ & + f \arctan\left(\frac{1}{\phi_2} \arctan\frac{x \sin 2\alpha + y \cos 2\alpha - 2 \sin \alpha}{x \cos 2\alpha - y \sin 2\alpha - 2 \cos \alpha}\right) \\ & = \text{const}, \end{aligned} \tag{5}$$

where  $f$  is the ratio of the flow strengths of the two jets and  $\phi_1$  and  $\phi_2$  are the angular half-widths of the flows within the two jets. For  $90^\circ$  collisions where  $f = 1$ ,  $\alpha = 45^\circ$ , and taking  $\phi_1 = \phi_2 \approx 0.2$  radian (due to the jets being more collimated in these experiments), one obtains the streamline distribution shown in Fig. 5(b). The experimental proton image is well simulated, with a narrow structure pointing in one direction and a much thicker one pointing in the opposite direction in the bisector plane. This asymmetry is a consequence of collisions of tilted jets, which result in formation of stronger field compression (denser streamlines) in the forward direction and weaker in the backward direction. Although collisionality may increase somewhat due to a lower energy in the center-of-mass frame, the jets

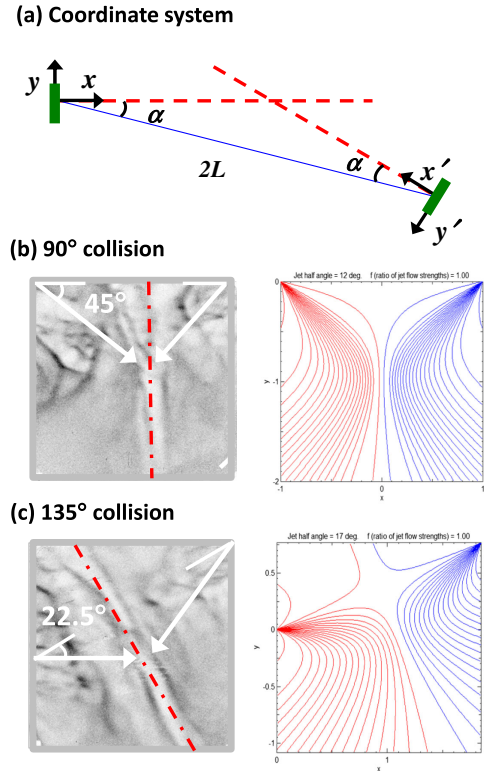


FIG. 5 (color online). Schematic drawing of coordinate system (a) to illustrate the collisions of two plasma jets at an angle =  $180^\circ - 2\alpha$ . Proton images of the collisions of two identical plasma jets (white arrows) is compared with model predicted streamlines of effective electron flow at  $90^\circ$  ( $\alpha = 45^\circ$ ) in (b) and  $135^\circ$  ( $\alpha = 22.5^\circ$ ) in (c), respectively. The dashed-dotted lines shown in the images indicate the bisector planes.

remain essentially collisionless. Figure 5(c) shows experimental images and analytic streamlines for pairs of equal plasma jets colliding at  $135^\circ$  ( $\alpha = 22.5^\circ$ ).

In summary, by combining proton images with numerical simulations and analytic modeling we have systematically studied the structure and dynamics of collisions of two laser-generated, high-Mach-number plasma jets at different angles. The result is novel physical insight into the interactions of two colliding plasma jets.

This work was supported in part by the U.S. DOE and LLE National Laser User's Facility (No. DE-FG52-07NA28 059 and No. DE-FG03-03SF22691), LLNL (No. B543881 and No. LDRD-08-ER-062), LLE (No. 414090-G), and FSC at the University of Rochester (No. 412761-G).

\*Corresponding author.

ckli@mit.edu

†Present address: Lawrence Livermore National Laboratory, Livermore, CA 94550, USA.

‡Present address: University of Michigan, Ann Arbor, MI 48109, USA.

- [1] D. D. Ryutov, N. L. Kugland, M. C. Levy, C. Plechaty, J. S. Ross, and H. S. Park, *Phys. Plasmas* **20**, 032703 (2013).
- [2] H. S. Park *et al.*, *High Energy Density Phys.* **8**, 38 (2012).
- [3] N. L. Kugland *et al.*, *Nat. Phys.* **8**, 809 (2012).
- [4] J. M. Foster, P. A. Rosen, B. H. Wilde, P. Hartigan, and T. S. Perry, *Phys. Plasmas* **17**, 112704 (2010).
- [5] G. Gregori *et al.*, *Nature (London)* **481**, 480 (2012).
- [6] S. Mondal *et al.*, *Proc. Natl. Acad. Sci. U.S.A.* **109**, 8011 (2012).
- [7] H. Ahmed *et al.*, *Phys. Rev. Lett.* **110**, 205001 (2013).
- [8] M. Borghesi, A. J. MacKinnon, A. R. Bell, R. Gaillard, and O. Willi, *Phys. Rev. Lett.* **81**, 112 (1998).
- [9] R. P. Drake, *High-Energy-Density Physics* (Springer, New York, 2006).
- [10] B. A. Remington, R. Drake, and D. Ryutov, *Rev. Mod. Phys.* **78**, 755 (2006).
- [11] D. R. Farley, K. Estabrook, S. Glendinning, S. Glenzer, B. Remington, K. Shigemori, J. Stone, R. Wallace, G. Zimmerman, and J. Harte, *Phys. Rev. Lett.* **83**, 1982 (1999).
- [12] J. M. Foster *et al.*, *Astrophys. J.* **634**, L77 (2005).
- [13] C. D. Gregory *et al.*, *Plasma Phys. Controlled Fusion* **50**, 124039 (2008).
- [14] S. V. Lebedev, *Astrophys. J.* **616**, 988 (2004).
- [15] P. A. Gourdain and C. E. Seyler, *Phys. Rev. Lett.* **110**, 015002 (2013).
- [16] Ph. Nicolai *et al.*, *Phys. Plasmas* **17**, 112903 (2010).
- [17] D. D. Ryutov, R. P. Drake, and B. A. Remington, *Astrophys. J.* **127**, 465 (2000).
- [18] D. D. Ryutov, B. A. Remington, H. F. Robey, and R. P. Drake, *Phys. Plasmas* **8**, 1804 (2001).
- [19] S. Ross *et al.*, *Phys. Plasmas* **19**, 056501 (2012).
- [20] A. Spitkovsky, *Astrophys. J.* **673**, L39 (2008).
- [21] T. N. Kato and H. Takabe, *Phys. Plasmas* **17**, 032114 (2010).
- [22] L. Gargate and A. Spitkovsky, *Astrophys. J.* **744**, 67 (2012).
- [23] D. D. Ryutov, *Astrophys. Space Sci.* **336**, 21 (2011).
- [24] R. Young *et al.*, *Bull. Am. Phys. Soc.* **58**, 245 (2013).
- [25] J. D. Lindl, *Phys. Plasmas* **2**, 3933 (1995).
- [26] C. K. Li *et al.*, *Science* **327**, 1231 (2010).
- [27] B. E. Blue *et al.*, *Phys. Rev. Lett.* **94**, 095005 (2005).
- [28] B. Loupias *et al.*, *Phys. Rev. Lett.* **99**, 205001 (2007).
- [29] D. D. Ryutov, N. L. Kugland, H.-S. Park, S. M. Pollaine, B. A. Remington, and J. S. Ross, *Phys. Plasmas* **18**, 104504 (2011).
- [30] J. M. Soures *et al.*, *Phys. Plasmas* **3**, 2108 (1996).
- [31] K. Shigemori *et al.*, *Phys. Rev. E* **62**, 8838 (2000).
- [32] C. D. Gregory, J. Howe, B. Loupias, S. Myers, M. M. Notley, Y. Sakawa, A. Oya, R. Kodama, M. Koenig, and N. C. Woolsey, *Astrophys. J.* **676**, 420 (2008).
- [33] D. D. Meyerhofer *et al.*, *Phys. Plasmas* **8**, 2251 (2001).
- [34] C. K. Li *et al.*, *Phys. Rev. Lett.* **102**, 205001 (2009).
- [35] M. Borghesi, A. Schiavi, D. H. Campbell, M. G. Haines, O. Willi, A. J. MacKinnon, P. Patel, M. Galimberti, and L. A. Gizzi, *Rev. Sci. Instrum.* **74**, 1688 (2003).
- [36] L. Willingale *et al.*, *Phys. Plasmas* **17**, 043104 (2010).
- [37] C. K. Li and Richard Petraso, *Phys. Rev. Lett.* **70**, 3059 (1993).
- [38] Away from the bisector plane, magnetic fields are nearly azimuthal around the jets and slowly varying with axial position; protons passing through this region experience deflection while approaching the jet that is nearly cancelled by an opposite deflection after passing the jet. Near the bisector plane, this cancellation does not occur because of rapid axial gradients and possibly chaotic structures. We also note that there is some angular spread in the directions of proton trajectories from the backlighter to the extreme edges of the imaged area, so the cancellations of deflections by the jets themselves, which is perfect only when the proton trajectory is almost perpendicular to the jet direction, is not perfect across the full width of the image; however, any effect of angular spread would be gradual across the image and would not explain the stark difference between the apparent structures near the bisector plane and away from it.
- [39] DRACO solves the two-dimensional radiation-hydrodynamic equation, assuming cylindrical symmetry. The electron-ion plasma is treated as a single fluid with separate electron and ion temperatures. Particle-collision effects are not included in the kinetic sense, and self-generated magnetic fields are not currently included in the simulations.
- [40] P. B. Radha *et al.*, *Phys. Plasmas* **12**, 056307 (2005).
- [41] M. J. Rosenberg, J. S. Ross, C. K. Li, R. P. J. Town, F. H. Séguin, J. A. Frenje, D. H. Froula, and R. D. Petraso, *Phys. Rev. E* **86**, 056407 (2012).
- [42] N. L. Kugland *et al.*, *Phys. Plasmas* **20**, 056313 (2013).
- [43] C. K. Li *et al.*, *Phys. Rev. Lett.* **97**, 135003 (2006).